Journal of Alloys and Compounds 509 (2011) 9249–9254

Contents lists available at ScienceDirect

Journal of Alloys and Compounds

journal homepage: www.elsevier.com/locate/jallcom

Synthesis of nanostructured Cu_xS thin films by chemical route at room temperature and investigation of their size dependent physical properties

A.U. Ubale[a,*], D.M. Choudhari[a], J.S. Kantale[a], V.N. Mitkari[a], M.S. Nikam[a], W.J. Gawande[a], P.P. Patil[b]

[a] Nanostructured Thin Film Materials Laboratory, Department of Physics, Govt. Vidarbha Institute of Science and Humanities, Amravati 444604, Maharashtra, India
[b] School of Physical Sciences, North Maharashtra University, Jalgaon, Maharashtra, India

ARTICLE INFO

Article history:
Received 31 December 2010
Received in revised form 1 July 2011
Accepted 5 July 2011
Available online 12 July 2011

Keywords:
Composite
Nanostructure
Electrical
Optical and structural properties

ABSTRACT

Nanostructured semiconductors show very interesting physical properties than bulk crystal due to size effects that arises because of quantum confinement of the electronic states. Using cupric acetate and sodium thiosulphate as cationic and anionic precursor, nanostructured Cu_2S thin films were successfully prepared at room temperature by chemical bath deposition technique. By varying the deposition time from 9 to 24 h, the Cu_2S films of thickness 70–233 nm were prepared. The different characterization methods such as X-ray diffraction (XRD), scanning electron microscopy (SEM), optical absorption and electrical resistivity measurement techniques were used to investigate size dependent properties of Cu_2S thin films. As thickness increases, the hexagonal covellite phase of CuS observed at thickness 70 nm gets converted to monoclinic chalcosite phase of Cu_2S. The resistivity and activation energy is found to be thickness dependent. The optical band-gap energy increases from 2.48 to 2.90 eV as thickness decreases from 233 to 70 nm. The influence of film thickness on carrier concentration, mobility and thermo-emf is reported.

1. Introduction

In recent years, nanostructured semiconductors are attracting research community in respect to their wide range of applications in opto and microelectronics [1–3]. The development of nanoscience and nanotechnology depends on the preparation and study of new nanoscale materials of improved properties and functionalities that forms building blocks for new devices. The surfaces and interfaces plays the critical roles in nanostructured materials as they have very high specific surface areas, and thus in their assembled forms there are large areas of interfaces. The fine grain size of the nanostructured material provides large number of atoms at edge and corner sites, which increases number of catalytically active sites. The chemical and physical properties of such materials are different as that of the bulk material. Among various metal chalcogenide semiconductor nanostructures, copper sulphide nanostructure has identified as a potential material for future applications in optoelectronic device like solar cells and fluorescent devices [4–11]. The copper sulphide has five stable phases: covellite (CuS), anilite ($Cu_{1.75}S$), digenite ($Cu_{1.8}S$), djurleite ($Cu_{1.95}S$) and chalcosite (Cu_2S) [12]. Several chemical and physical techniques have been investigated to prepare different phases of Cu_xS. Varkey [13] has reported deposition of Cu_xS using EDTA as a complexing agent in a bath comprising CuCl, NaC1 and hydroxylamine hydrochloride solutions. Sagade and Sharma [14] have used solution growth technique to deposit Cu_xS ($x = 1$, 1.4, and 2) thin films on glass substrates at room temperature (300 K). The physico-chemical properties of the films are highly influenced by the chemical composition. Nair et al. [15] have reported the optoelectronic and solar control properties of chemically deposited Cu_xS thin films. Lindroos et al. [16] have prepared copper sulphide thin films by successive ionic layer adsorption and reaction method at room temperature. The films were polycrystalline and showed no preferred orientation. Bezig et al. [17] have used vacuum evaporation technique to prepare Cu_xS thin films. Fatas et al. [18] have used $CuSO_4$ and thiourea in alkaline medium to deposit Cu_xS thin films by chemical method and reported that their optical band-gap and resistivity is of the order of 2.58 eV and 3×10^{-3} Ω cm, respectively.

To the best of our knowledge, no report is available on the effect of film thickness on the physical properties of Cu_xS. For the present work, we have chosen chemical bath deposition (CBD) method for the preparation of nanostructured Cu_xS thin films at room temperature, which is simple and economic. The CBD method involves "bottom up" approach in which the nanostructures are built up by ion-by-ion or cluster-by-cluster condensation of the precipitate on the substrate [19]. The easy control on the various deposition parameters like deposition time, pH of the bath, ionic concentration etc. can be achieved in CBD method to deposit binary and ternary nanostructured semiconductor materials on the substrate

* Corresponding author. Tel.: +91 721 2531706; fax: +91 721 2531705.
E-mail address: ashokuu@yahoo.com (A.U. Ubale).

0925-8388/$ – see front matter © 2011 Elsevier B.V. All rights reserved.
doi:10.1016/j.jallcom.2011.07.009

[20,21]. As growth process follows ion-by-ion or cluster-by cluster deposition, high surface areas can be attained either by fabricating small particles or clusters where the surface-to-volume ratio of each particle is high, or by creating materials having porous surface. The focus of this study is to develop a general and low-cost solution-based process to prepare nanostructured Cu_xS thin films and describe how the film thickness affects its physical properties.

2. Experimental

The chemical bath deposition (CBD) technique is one of the simple and economic bottom-up technique to deposit a wide variety of binary, ternary and composite thin films. In CBD process, the cleaning of the substrate is very important as it affects the film growth process remarkably. The glass substrates of size (25.4 mm × 75 mm × 1.2 mm) supplied by Blue Star, Mumbai, were initially boiled in chromic acid for 30 min and kept in it for next 48 h at room temperature. The slides were then dipped in labolene detergent and washed with double distilled water. The substrates were further dipped in AR grade acetone and dried for 15 min, prior to the deposition. An aqueous solution of cupric acetate and sodium thiosulphate was used as cationic and anionic precursor. 30 ml of 0.1 M cupric acetate ($C_3H_6CuO_4{\cdot}H_2O$) and 30 ml of 0.1 M sodium thiosulphate ($Na_2S_2O_3{\cdot}5H_2O$) solutions were added to the beaker kept at room temperature. Then the concentrated HCL was added drop wise in the reaction mixture to adjust pH to 4. The prepared solution was stirred continuously for 5 min and then cleaned glass substrates were immersed into this final solution. The solution colour was changed to golden brown after about 30 min, which indicates initiation of the chemical reaction. The substrates were removed after fix interval of time from the bath, washed with the distilled water, and dried in a stream of nitrogen gas. For thin film characterization, the sensitive microbalance was used to measure film thickness using the relation:

$$t = \frac{m}{A\rho} \quad (1)$$

where m is the mass of the film deposited on the substrate which covers area A (cm^2) and ρ is density of the material in bulk form ($\rho \approx 5.6\ g/cm^3$). For the structural, surface morphological and optical characterizations of Cu_xS thin films, the X-ray diffraction (XRD), scanning electron microscopy (SEM) and UV–vis spectrophotometer techniques were used. During X-ray scanning, Cu Kα radiation of wavelength 0.154 nm was used. Optical absorption study was carried out in the wavelength range 310–1100 nm. The two-point dc probe method of dark electrical resistivity was used to study the variation of resistivity with temperature. A rectangular copper block was used as a sample holder and chromel–alumel thermocouple was used to measure the temperature. For the thermoelectric power measurement, the open circuit thermo-voltage generated by the sample, when a temperature gradient is applied across the length of the sample was measured using a digital microvoltmeter. Hall effect setup supplied by Scientific Equipments, Roorkee, India was used for the measurements of electrical parameters, carrier concentration (n) and mobility (μ) at room temperature. Specially designed Hall probe on printed circuit board (PCB) was used to fix the sample of the size 10 mm × 10 mm such that the gaps between current and voltage probes are around 3 and 7 mm, respectively. Silver paste was employed to ensure good electrical contacts. Van der Pauw technique [22–24] was used for this purpose.

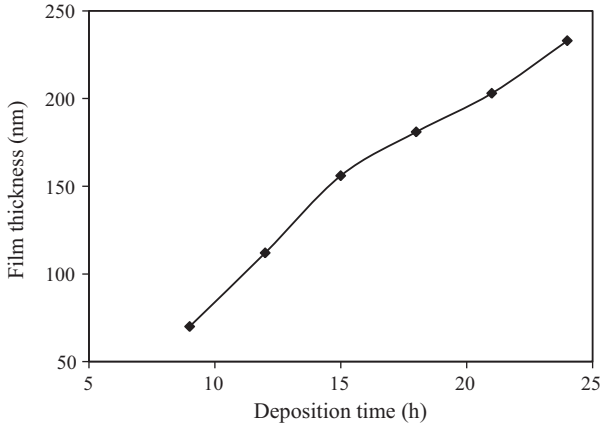

Fig. 1. Variation of Cu_2S film thickness with deposition time.

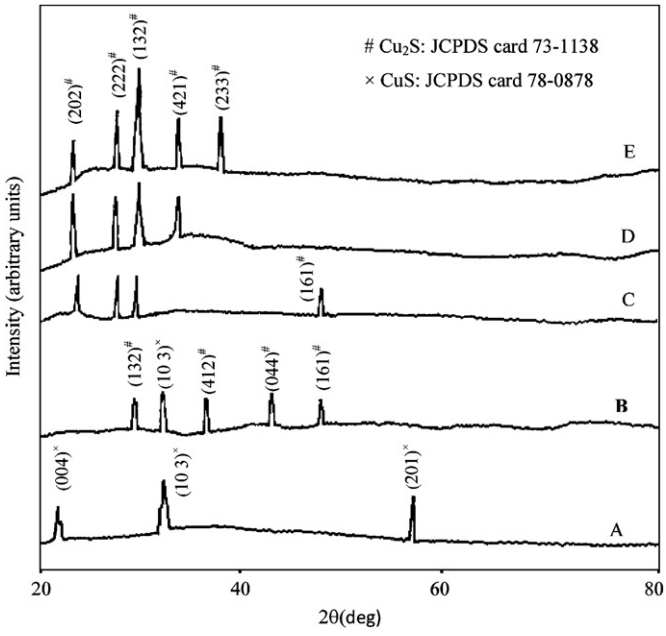

Fig. 2. X-ray diffraction pattern of Cu_2S thin film of thickness: (A) 70 nm, (B) 112 nm, (C) 156 nm, (D) 181 nm and (E) 203 nm.

3. Results and discussion

3.1. Cu_xS growth mechanism

Chemical bath deposition is a novel and economical process for the production of nanostructured particles of the composite chalcogenides for advanced device applications. Cu_xS thin films were deposited by decomposition of sodium thiosulphate and cupric acetate in acidic solution. The deposition process is based on the slow release of Cu^{2+} and S^{2-} ions in the solution, which condenses on the substrate, by ion-by-ion or cluster-by-

Table 1
Comparison of observed XRD data of thin films with the JCPDS cards (Cu_2S: 73-1138 and CuS: 78-0878).

Film thickness (nm)	Observed values		Standard value		hkl	Phase
	2θ (°)	d (Å)	2θ (°)	d (Å)		
A 70 nm	21.87	4.110	21.929	4.050	004	CuS
	32.00	2.794	32.072	2.788	103	CuS
	56.72	1.640	56.784	1.619	201	CuS
B 112 nm	29.33	3.035	29.215	3.054	132	Cu_2S
	32.11	2.785	32.072	2.788	103	CuS
	36.22	2.422	36.219	2.478	412	Cu_2S
	42.66	2.120	42.634	2.118	044	Cu_2S
	47.40	1.916	47.418	1.915	161	Cu_2S
C 156 nm	23.50	3.763	23.534	3.777	202	Cu_2S
	28.03	3.183	27.968	3.187	222	Cu_2S
	29.25	3.055	29.215	3.054	132	Cu_2S
	47.40	1.921	47.418	1.915	161	Cu_2S
D 181 nm	23.48	3.766	23.534	3.777	202	Cu_2S
	27.92	3.184	27.968	3.187	222	Cu_2S
	29.24	3.098	29.215	3.054	132	Cu_2S
	33.80	2.664	33.795	2.650	421	Cu_2S
E 203 nm	23.54	3.775	23.534	3.777	202	Cu_2S
	28.00	3.176	27.968	3.187	222	Cu_2S
	29.31	3.064	29.215	3.054	132	Cu_2S
	33.81	2.649	33.795	2.650	421	Cu_2S
	38.04	2.365	37.998	2.366	233	Cu_2S

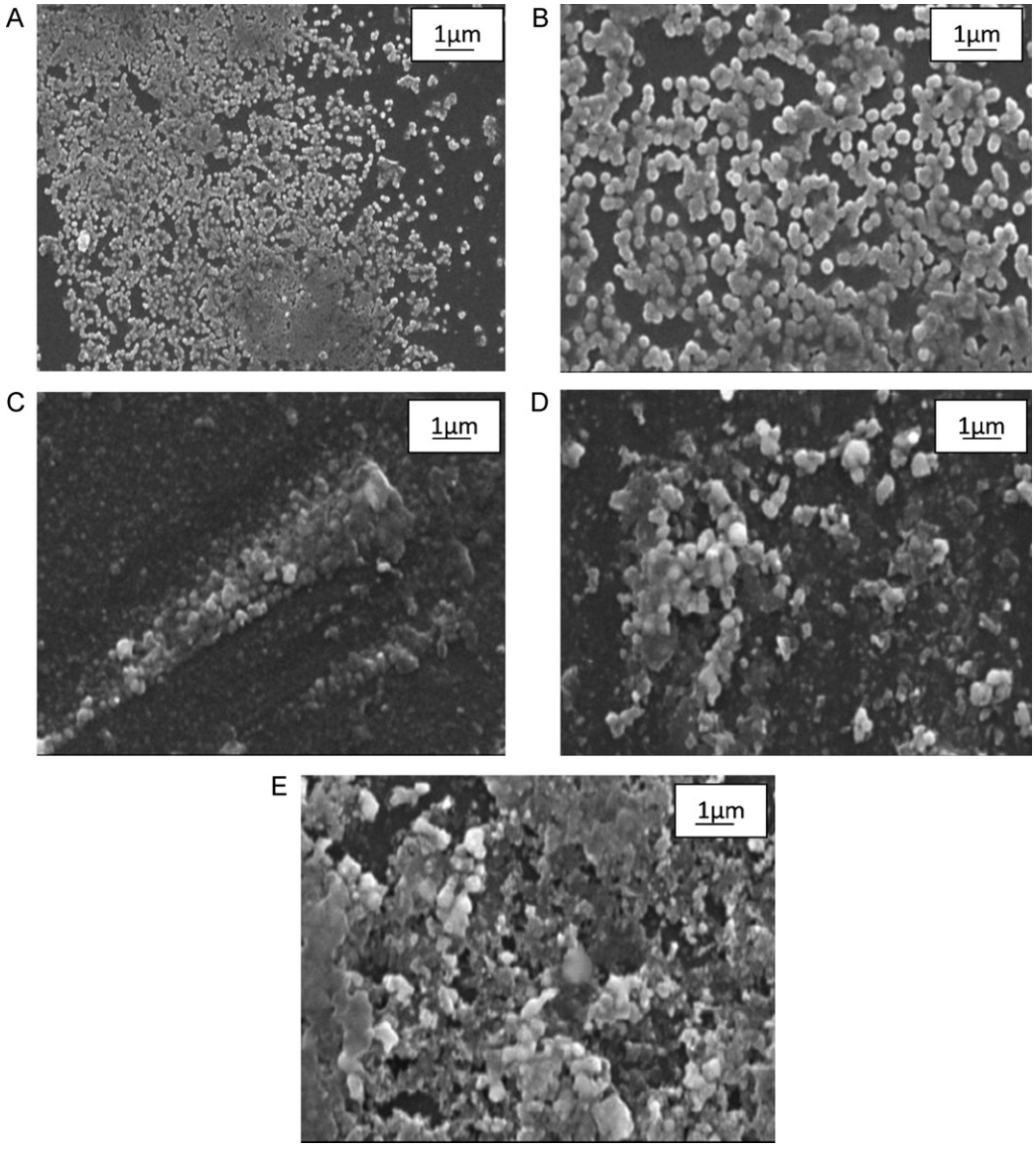

Fig. 3. SEM images of Cu_2S thin films: (A) 70 nm, (B) 112 nm, (C) 156 nm, (D) 181 nm and (E) 203 nm.

cluster process. When the solution is saturated, ionic product is equal to the solubility product and when it exceeds, precipitation occurs and ions condense on the substrate and in the solution to form nuclei. The deposition takes place when the ionic product of Cu^{2+} and S^{2-} is greater than the solubility product. Ion-by-ion or cluster-by-cluster deposition takes place depending upon the preparative conditions such as bath temperature, pH and solution concentration [19,25,26]. In the present case, deposition was carried out for fix interval of deposition time at room temperature. Fig. 1 shows variation of film thickness with deposition time. The film thickness increases with deposition time. During the deposition process, it was observed that the clear transparent solution slowly changed to golden brown and then rapidly became dark at around 15 h deposition time and finally transferred into nearly colourless above 25 h. This indicates that growth rate slowly rises and becomes 10.40 nm/h around 15 h, where the process reaches to the saturation stage and thereafter the growth rate slowly decreases with time. This is mainly due to decrease in the concentration of reactant with time.

3.2. Structural characterization

Structural identification of Cu_xS films were carried out from the analysis of the X-ray diffractogram taken in the range of 2θ between 20 and 80°. The XRD patterns of the Cu_xS films of various thicknesses deposited on glass substrates are shown in Fig. 2. Table 1 summaries the crystallographic data of these films compared with standard JCPDS data files, Cu_2S: 73-1138 and CuS: 78-0878. The analysis showed that film of thickness 73 nm is nanocrystalline in nature with hexagonal covellite phase of CuS. Well defined (0 0 4), (1 0 3) and (2 0 1) peaks are observed in the XRD pattern due to covellite phase. However, the film of thickness 112 nm consists mixed phase of covellite CuS and chalcosite Cu_2S. At 112 nm film thickness the (1 0 3) is retained and other orientations (1 3 2), (4 1 2), (0 0 4) and (1 6 1) are appeared due to Cu_2S monoclinic chalcosite phase. After 112 nm film thickness, the films are oriented in the (1 3 2) direction showing single chalcosite phase of Cu_2S. Here it is important to point out that, the XRD patterns of Cu_xS distinguishes itself from the hexagonal CuS and monoclinic Cu_2S phases depending on film thickness. Because of copper enrichment in CuS with

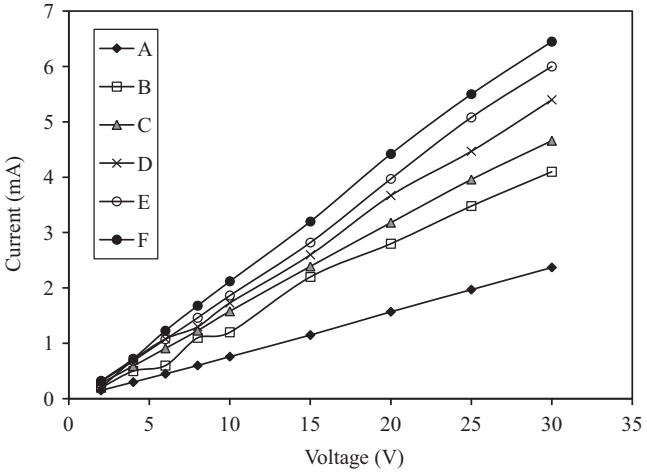

Fig. 4. *I–V* characteristic of Cu_2S thin films: (A) 70 nm, (B) 112 nm, (C) 156 nm, (D) 181 nm, (E) 203 nm and (F) 233 nm.

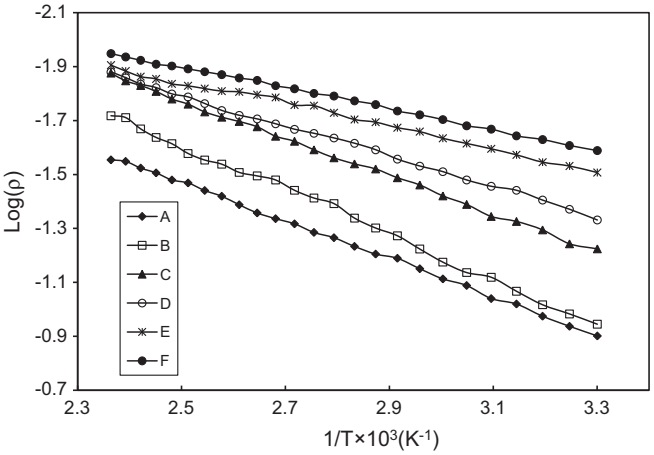

Fig. 5. Variation of log (ρ) vs. $1/T \times 10^3$ (K^{-1}) for Cu_2S films with different thickness: (A) 70 nm, (B) 112 nm, (C) 156 nm, (D) 181 nm, (E) 203 nm and (F) 233 nm.

minor rearrangements of the sulphur atoms, the Cu_xS changes its crystal structure from CuS to Cu_2S. In deposition-bath sodium thiosulphate dissociates immediately in the distilled water to release sulphur ions. However, the cupric acetate dissociates slowly in the beginning to release copper ions to react with sulphur as it was observed that the solution colour was slowly changed to golden brown in the beginning up to 10 h deposition time and after that it rapidly become dark golden brown. The average crystallite size of the film was determined by using Scherrer formula:

$$d = \frac{0.9\lambda}{\beta \cos\theta} \tag{2}$$

where λ is the wavelength used (1.54 Å); β is the angular line width at half maximum intensity in radians; θ is the Bragg's angle. It was found that crystallite size increases from 7 to 33 nm as film thickness increases from70 to 233 nm.

3.3. SEM studies

Scanning electron microscopy was used to study the surface morphology of the sample. The SEM micrographs of Cu_xS thin films are shown in Fig. 3. In the initial stage of film growth, the surface shows circular islands, which are multiple nucleation centers with lot of empty spaces between them. When the thickness of the Cu_xS thin film increases, small islands grew up and coalescence of the islands occurred. After thickness 156 nm surface of the film was quite rough and well covered by the densely packed nanocrystals with improved grain size. Around 112 nm to 156 nm thickness, the film surface is smooth and nonporous but above 181 nm thickness, film surface becomes quite porous due to irregular overgrowth of the material. This was also supported by the fact that the solution colour during deposition process was changed very slowly in the beginning indicating slow reaction rate up to film thickness 112 nm, i.e. up to 12 h. That is why up to thickness 112 nm the moderate growth rate gives birth to circular and well-defined islands and above that thickness the film surface shows porous and rough surface due to enhanced reaction rate.

3.4. Electrical resistivity

The current–voltage (*I–V*) characteristics of the films were studied in dark to check nature of the Cu_xS/Ag contact using two-probe method. The *I–V* characteristics for Cu_xS thin films are found to be linear, which shows that silver produces ohmic contacts with it. Fig. 4 shows that current flowing through the film increases with thickness, which may be due to improvement in crystallite structure. At 30 V, current flowing through the film of thickness 70 nm was 2.37 nA and rises to 6.45 nA for the film of thickness 233 nm.

The variation of dark electrical resistivity of Cu_xS films of different thicknesses were studied in the temperature range 303–423 K using dc two-point probe method (Fig. 5). It was seen that resistivity decreases with rise in temperature indicating semiconducting nature of Cu_2S. The resistivity of Cu_xS decreases as film thickness increases. It may be because grain size improves from 7 to 33 nm as film thickness increases from70 to 233 nm [27,28]. At lower thickness, the film surface is covered by circular islands with lot of empty spaces between them producing large number of grain boundaries and discontinues in the film as a result they show more resistivity at lower thickness. Above thickness 112 nm, these islands continued to grow into bigger grains showing overgrowth on the surface that reduces the resistivity. The variation in electrical conductivity with film thickness at temperature 373 K is given in Fig. 6. The conductivity of Cu_xS thin film decreases from 1.75 to 0.66 $\Omega\,cm^{-1}$ as the film thickness varies from 70 to 233 nm. The thermal activation energy was calculated using the relation:

$$\rho = \rho_0 \exp\left(\frac{E_0}{KT}\right) \tag{3}$$

where ρ is resistivity at temperature T, ρ_0 is a constant, K is Boltzmann constant (8.62×10^{-5} eV/K) and E_0 is the activation energy required for conduction. The activation energy decreases from 0.16 to 0.08 eV as film thickness varies from 70 to 233 nm (Fig. 7). At lower thickness, the film has large empty voids so that an electron may need more energy to tunnel from one island to other giving high activation energy as that of thick film.

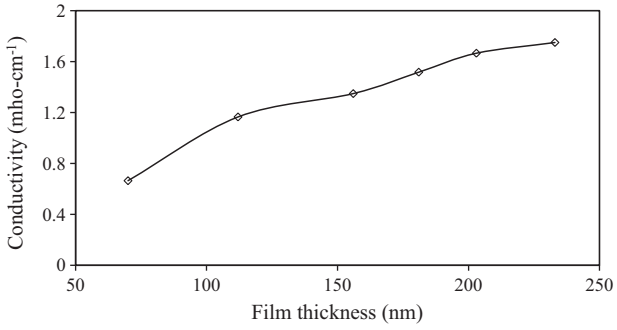

Fig. 6. Variation of electrical conductivity at 303 K temperature of Cu_2S with film thickness.

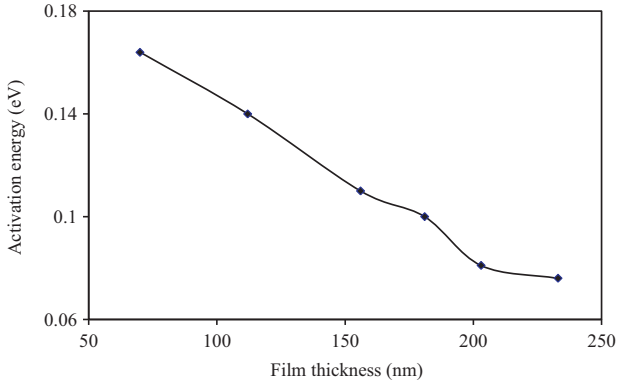

Fig. 7. Variation of activation energy of Cu_2S with film thickness.

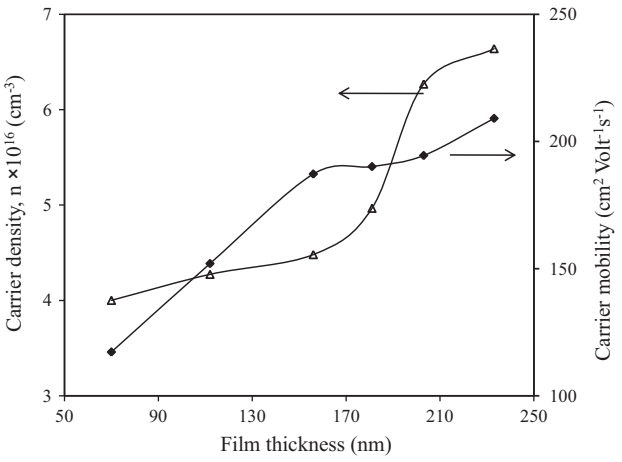

Fig. 8. Variation of carrier density and mobility of Cu_2S with film thickness.

The Hall measurements were carried out using a four-probe technique to measure mobility and carrier concentration. The carrier density and Hall mobility determined were found thickness dependant. Both carrier density and mobility increase with film thickness (Fig. 8). Carrier concentration is of the order of 10^{16} cm^{-3} and it increases rapidly up to film thickness 156 nm and then slowly for further rise in thickness. The increased carrier concentration can be related to the observed improvement in crystallinity of the Cu_xS thin films with thickness due to agglomeration of islands to give pinhole free surface as seen in SEM of the film of thickness 156 nm. After 156 nm carrier concentration rises slowly with thickness as porous overgrowth is observed. The mobility of carriers also linearly rises up to thickness 156 nm and once the surface of the substrate was fully covered by Cu_xS it rises rapidly up to 181 nm thickness and thereafter slowly as porosity of the film increases.

The thermoelectric power measurement was used to determine the type of conductivity. The temperature difference between the two ends of the sample causes transport of carriers from the hot to cold end, thus creating an electric field, which shows thermo-emf across the ends. The thermo-emf generated is directly proportional to the temperature gradient maintained across the semiconductor ends as well as to the film thickness. At 433 K temperature difference applied across the ends of the sample the generated emf was 3.04 mV and it increases to 5.02 mV as film thickness varied from 70 to 233 nm (Fig. 9). The type of conductivity was decided from the sign of the emf generated at the cold and hot end. In the case of Cu_xS thin films studied by us the negative terminal was found to be at the hot end; therefore, the film shows p-type conduction mechanism.

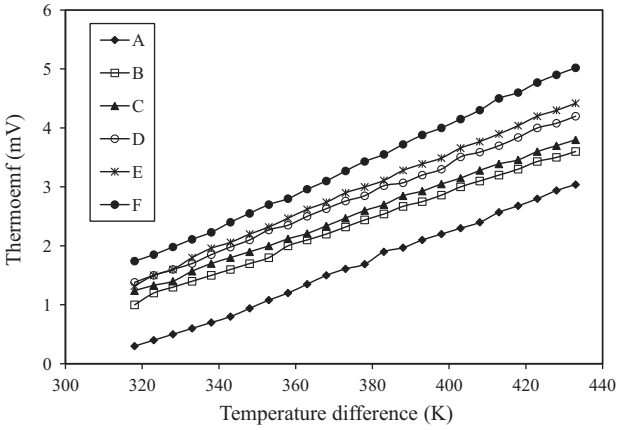

Fig. 9. Plots of thermo emf versus temperature difference of Cu_2S thin films of various thickness: (A) 70 nm, (B) 112 nm, (C) 156 nm, (D) 181 nm, (E) 203 nm and (F) 233 nm.

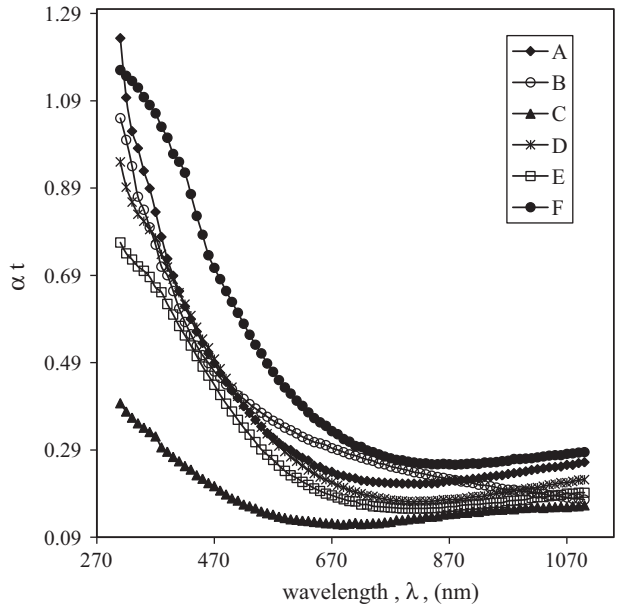

Fig. 10. Variation of optical absorption, αt with wavelength, λ of Cu_2S thin films of different thickness: (A) 70 nm, (B) 112 nm, (C) 156 nm, (D) 181 nm, (E) 203 nm and (F) 233 nm.

3.5. Optical properties

Optical properties of the Cu_xS films were studied from the absorption spectra measured by a UV–vis–NIR spectrometer in the wavelength range 310–1100 nm. The absorption spectra for the Cu_xS thin films of different thicknesses deposited on glass substrates are shown in Fig. 10. At incident wavelength 310 nm the absorption coefficient of the film of thickness 70 nm is 4.97×10^4 cm^{-1} and it increases to 17.6×10^5 cm^{-1} at 233 nm thickness. From the absorption spectra, the optical band-gaps of the films of different thickness were calculated using the fundamental absorption relation, which corresponds to electron excitation from the valance band to conduction band. The absorption coefficient (α) and the incident photon energy ($h\nu$) are related by the equation [29,30]:

$$\alpha h\nu = A(h\nu - E_g)^n \quad (4)$$

where $h\nu$ is the photon energy, E_g is the band gap energy, A and n are constants. For allowed direct transitions $n = 1/2$ and for allowed

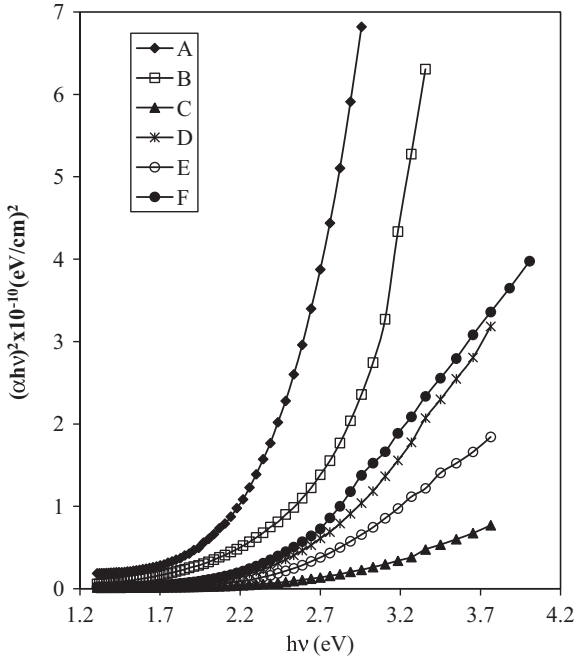

Fig. 11. Plots of $(\alpha h\nu)^2$ versus $h\nu$ for Cu_2S thin films of different thickness: (A) 70 nm, (B) 112 nm, (C) 156 nm, (D) 181 nm, (E) 203 nm and (F)233 nm.

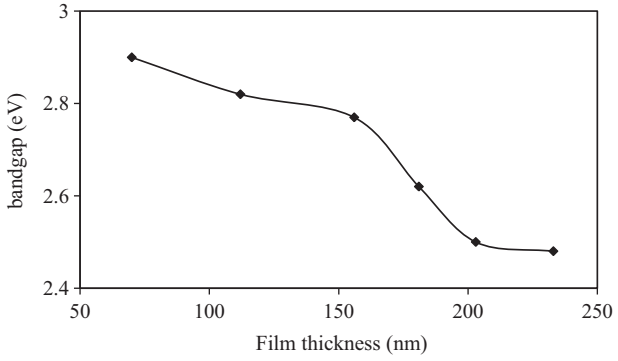

Fig. 12. Variation of band-gap energy of Cu_2S with film thickness.

indirect transitions $n = 2$. Taking $n = 1/2$, the direct optical band-gap is calculated from $(\alpha h\nu)^2$ vs. $h\nu$ plot (Fig. 11) by extrapolating the linear portion of the graph to $h\nu$ axis. The intercept on the $h\nu$ axis determines the direct band-gap. Fig. 12 shows the variation of the optical-band gap energy of Cu_xS film with thickness. The energy gap increases from 2.48 to 2.90 eV with decrease in film thickness from 233 to 70 nm. The red shift in the absorption edge of Cu_xS thin film is associated with the smaller grain size of the nanostructured material as the different size effects becomes prominent in it.

4. Conclusions

Nanostructured Cu_xS thin films were prepared onto glass substrates by the CBD technique in an aqueous medium. The X-ray diffraction study reveals that depending on thickness, the hexagonal covellite phase of CuS observed at thickness 70 nm gets converted to monoclinic chalcosite phase of Cu_2S at higher thickness due to enrichment of copper. The SEM images shows circular islands with lot of empty spaces at lower thickness, which grew up to produce porous material at higher thickness. The resistivity, activation energy and optical band gap of Cu_xS thin films were found thickness dependent. The measurement of thermo-emf confirms p-type conduction mechanism of Cu_xS. The influence of film thickness on carrier concentration and mobility of Cu_xS is also reported.

Acknowledgement

The authors are thankful to University Grants Commission, WRO, Pune (India), for financial support under the project (No. F47-1695/10).

References

[1] S. Kaci, A. Keffous, M. Trari, H. Menari, A. Manser, J. Alloys Compd. 496 (2010) 628.
[2] S. Mann, Nature 322 (1988) 119.
[3] S. Karan, B. Mallik, Nanotechnology 19 (2008) 495202.
[4] S.D. Sartale, C.D Lokhande, Mater. Chem. Phys. 65 (2000) 63.
[5] S. Lindroos, A. Arnold, M. Leskela, Appl. Surf. Sci. 158 (2002) 75.
[6] I. Grozdanov, M. Najdoski, J. Solid State Chem. 114 (1995) 469.
[7] S. Dhar, S. Chakraborti, J. Appl. Phys. 82 (1997) 655.
[8] G. Nickless, Inorganic Chemistry of Sulfur , Elsevier, London, 1968, p. 670.
[9] N.N. Greenwood, E.A. Earnshaw, Chemistry of the Elements , Pergamon, Oxford, 1990, p. 1403.
[10] L.D. Partain, R.A. Schneider, L.F. Donaghey, P.S. Mcleod, J. Appl. Phys. 57 (1985) 5056.
[11] P.K. Nair, M.T.S. Nair, J. Phys. D 24 (1991) 83.
[12] H.M. Pathan, J.D. Desai, C.D. Lokhande, Appl. Surf. Sci. 202 (2002) 47.
[13] A.J. Varkey, Sol. Energy Mater. 19 (1989) 415.
[14] A.A. Sagade, R. Sharma, Sens. Actuators B 133 (2008) 135.
[15] P.K. Nair, V.M. Garcia, A.M. Fernandez, H.S. Ruiz, M.T.S. Nair, J. Phys. D: Appl. Phys. 24 (1991) 441.
[16] S. Lindroos, A. Arnold, M. Leskel, Appl. Surf. Sci. 158 (2002) 75.
[17] B. Bezig, S. Duchemin, F. Guastavino, Sol. Energy Mater. 2 (1979) 53.
[18] E. Fatas, T. Garcia, C. Ontemoyer, A. Media, E.G. Camerevo, F. Arjona, Mater. Chem. Phys. 12 (1985) 121.
[19] A.U. Ubale, Mater. Chem. Phys. 121 (2010) 555.
[20] E. Rabinovich, E. Wachtel, G. Hodes, Thin Solid Films 517 (2008) 737.
[21] A.U. Ubale, S.C. Shirbhate, J. Alloys Compd. 497 (2010) 228.
[22] L.J. Van der Pauw, Philips Res. Rep. 13 (1958) 1.
[23] H.L. Chen, Y.M. Lu, W.S. Hwang, Surf. Coat. Technol. 198 (2005) 138.
[24] A.V. Moholkar, S.M. Pawar, K.Y. Rajpure, C.H. Bhosale, J.H. Kim, Appl. Surf. Sci. 255 (2009) 9358.
[25] G. Godes, Chemical Solution Deposition of Semiconductor Films , Marcel Dekker, 2003.
[26] H.E. Esparza-Ponce, J. Hernandez-Borja, A. Reyes-Rojas, M. Cervantes-Sanchez, Y.V. Vorobiev, R. Ramirez-Bon, J.F. Perez-Robles, J. Gonalez-Hernandez, Mater. Chem. Phys. 113 (2009) 824.
[27] A.U. Ubale, D.K. Kulkarni, Bull. Mater. Sci. 28 (1) (2005) 43.
[28] A.U. Ubale, D.K. Kulkarni, Ind. J. Pure Appl. Phys. 44 (2006) 254.
[29] J.I. Pankove, Optical Processes in Semiconductors , Prentice-Hall Inc., Englewood Cliffs, NJ, 1971, p. 34.
[30] S.S. Shinde, P.S. Shinde, C.H. Bhosale, K.Y. Rajpure, Solid State Sci. 10 (9) (2008) 1209.